THE FLUMIC ELECTRON ENVIRONMENT MODEL

D.J. Rodgers
Space Department, QinetiQ
Farnborough, GU14 0LX, UK
Phone: +44-1252-394297
Fax: +44-1252-396330
E-mail: djrodgers@space.qinetiq.com

K.A. Hunter
QinetiQ

G.L. Wrenn
Retired from Space Department, DERA

Abstract

Assessments of the vulnerability of spacecraft materials to internal charging need a good electron environment model. Since the threat from electrostatic discharges is related to the occurrence of flux enhancements, the standard mean flux models are not appropriate. The requirement is for a model of enhanced flux conditions. These tend to occur mainly during the declining phase of the solar cycle.

FLUMIC (Flux Model for Internal Charging) was written to address this requirement. The model was originally developed as a simple engineering tool. Although simplicity of use is still the philosophy behind FLUMIC, it has undergone improvements to its accuracy and scope, mainly through the inclusion of better data sets and more sophisticated empirical modelling techniques. The latest version, FLUMIC3, has been developed in a new ESA study and relies heavily on data from the GOES/SEM and STRV-1b/REM instruments.

Although the outer belt, including geostationary orbit, is the region most at risk from internal charging effects, charging currents in the inner belt are not insignificant behind thin shields. The model now extends to the inner belt so that the current contributions from both inner and outer belts can be considered for satellites in eccentric orbits.

FLUMIC can be used as a tool in its own right but is also incorporated in the DICTAT internal charging tool. FLUMIC3 will be included in a new version of DICTAT to be released shortly.

Introduction

Internal charging is a well-established hazard that spacecraft designers must protect against and numerous design guidelines have been established, e.g. [1] for its mitigation. Energetic electrons that penetrate into dielectric materials lead to a build-up of charge. Grounded conductive components immediately leak away any deposited charge and so are safe from this process. However, ungrounded conductors collect charging in the same way as dielectrics and will be susceptible to ESD through intermediate insulators.

Although the fluxes of penetrating electrons are small, enhancements are long-lasting. In geostationary orbit outer belt enhancements may persist for several days. This is long enough

for strong electric fields to develop within dielectrics and between ungrounded conductors and other materials. As a result, there is the possibility of electrostatic discharge, which causes damage to sensitive electronics. There is clear evidence to indicate that many satellite systems have been degraded or destroyed by this process [2].

Protection by means of circuit desensitisation, careful component placement and shielding is possible but its implementation and validation can be time consuming and it adds cost to a mission. It is therefore important that unnecessary caution is avoided. There are long-established 'AE' and 'AP' series of electron and proton environment models for use in radiation calculations, of which AE-8 is the most recent electron model. This is a model of mean fluxes as a function of location, defined by B and L.. While this is useful for total dose calculations, it is inappropriate for the calculation of internal charging risk which is a function of temporary enhancements. Figure 1 shows the variability of daily averages of geostationary >2MeV electron flux in 1994, compared to the flux expected from the AE8 model.

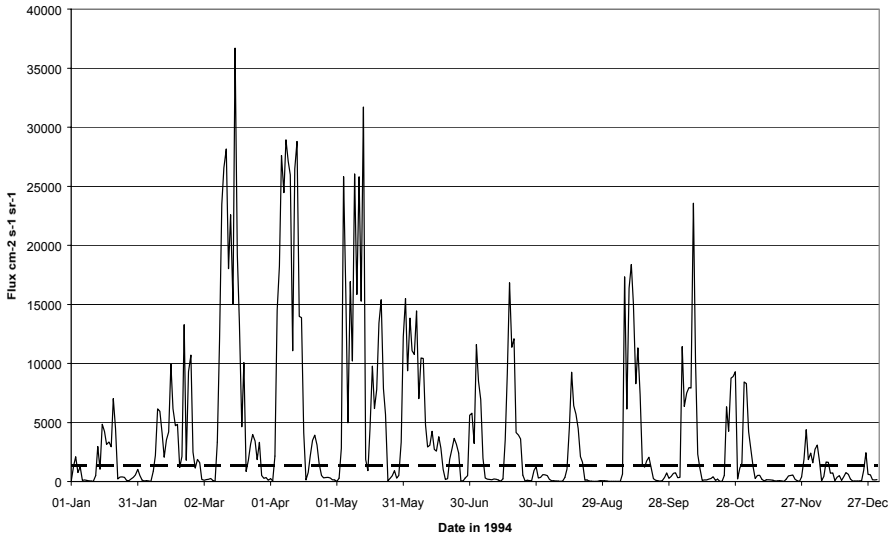

Figure 1. Daily-averaged >2MeV electron flux in geostationary orbit for 1994 as seen by GOES-7 compared to the AE-8 MIN model (dashed line).

A suitable severe case is needed by designers to use in risk assessment. Such a severe case is provided by FLUMIC (Flux Model for Internal Charging) described in this paper.

The 'Worst Case' Environment

It is common practice for designers to work to worst case specifications. However, this concept is often hard to define in practice. For internal charging, higher fluxes with energy sufficient to pass through spacecraft shielding lead to greater current deposited in internal dielectrics. However, such enhancements may be accompanied by a hardening of the electron energy spectrum which causes increased dose-rate, increase radiation-induced conductivity and a tendency to reduce charging. The balance between these competing effects depends on the properties of the material concerned. Also, a high flux for a brief period may be less hazardous than a lower flux for a longer period. Again this is material dependent. Hence there is no environment that is a worst case for all materials.

Characteristics of the FLUMIC Model

The characteristics of the model are defined to make it a severe environment generally applicable to all materials. These characteristics are:

- based on daily averages of flux – because only materials with a charging time-scale of 1 day or more are capable of charging to high levels.
- based on extreme flux levels at >2MeV – because high flux at this energy is most specifically associated with known spacecraft anomalies.
- based on the mean spectrum for the extreme flux level – because this leads to the most general severe case.

Other characteristics:

- conservative i.e. observed fluxes will virtually always be below that of the model.
- based on physical quantities, L and B/B0.
- most accurate where this is warranted. This means accurate at geostationary orbit where most spacecraft reside. For other orbits, it is most accurate near the magnetic equator, where fluxes are most intense. Accurate modelling of low-flux regions, e.g. near the atmospheric cut-off, is unnecessary.
- reflecting seasonal and solar cycle variations.

The Series of FLUMIC Models

FLUMIC was first created in 1998 [3] and was updated to FLUMIC2 in 2000 [4]. Both these versions of the code modelled the outer electron belt only. This latest version, FLUMIC3, updates the outer belt electron model and also models electron fluxes in the inner belt. Whilst internal charging has not been observed to be a problem for spacecraft confined to the inner belt, the extension of the model is to permit better assessment of eccentric orbits which encounter both inner and outer belt fluxes. All of the versions of FLUMIC have been designed to be used within the DICTAT [5] internal charging tool. However, FLUMIC can be used to provide input to other types of analysis and DICTAT can take other environment specifications as input. FLUMIC3 will be included in a new version of DICTAT to be released in 2004.

Data sources

FLUMIC3 is based heavily on data from the GOES/SEM [6] and STRV-1b/REM [7] instruments. This has is augmented in the inner belt by the short-lived STRV-1d/SURF [8] instrument because of its resistance to proton contamination.

GOES/SEM – Long-term seasonal and solar cycle behaviour of geostationary fluxes

STRV-1b/REM – Outer belt profiles and seasonal variation
STRV-1d/SURF & STRV-1b/REM – Inner belt profiles

The characteristics of these three databases are summarised in Table 1.

Other data sources have been used to provide confirmation of the these data sets. None of the data sets provided sufficient information away from the geomagnetic equator for this

variation to be explicitly modelled. Instead, the flux attenuation away from the equator was based on theoretical extrapolations.

Table 1. Summary of databases used for FLUMIC

REM	Orbit	GTO with inclination of 7˚
	Data duration	1994 to 1998.
	Data	Electron flux in three channels, 1-2.2 MeV, 2.2-4.6 MeV and 4.6-10 MeV
GOES	Orbit	Geostationary, with longitude around 75W and 135W.
	Data duration	More than a solar cycle
	Data	Electron flux in two channels, >0.6MeV and >2MeV.
SURF	Orbit	GTO, with inclination of 7˚
	Data duration	12 days, after which communication with the spacecraft was lost.
	Data	Electron current behind two levels of shielding, corresponding approximately to 1MeV and 1.7MeV

Cross- Calibration Issues

Effect of magnetic field co-ordinates

Cross calibration between different data sources can only be done at the same value of L and B/B0. In geostationary orbit, the gradient of flux in L is very steep and hence a spacecraft sees a significant variation in flux, due to the variation in L (typically L=6.6 to 7.5) caused by the pressure of the solar wind. The diurnal variation in L varies strongly with geomagnetic activity, as is exhibited by the Tsyganenko 1989 [9] model. An example of the effect on a typical geostationary satellite is plotted in Figure 2 below.

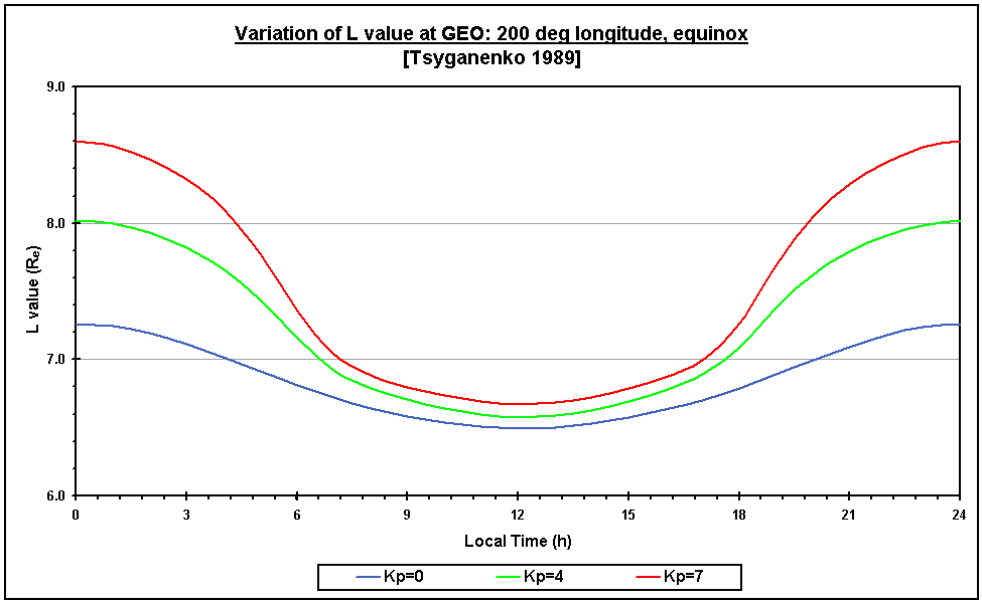

Figure 2. Diurnal variation of L value, as modelled by the Tsyganenko 1989 [9] model.

Figure 2 shows that L is least affected by changes in the shape of the magnetosphere around local noon. At this location, it makes little difference which level of geomagnetic activity is assumed. In the construction of FLUMIC3, a quiet-time (Kp=0) has been adopted.

This can be justified because it will lead to a safe over-estimation of flux and its effects will be limited because the intervals of substorm field distortion are generally short compared to the charge build-up times required to produce hazardous discharge. Very large, long-lasting geomagnetic storms can be considered separately.

GOES/GOES cross-calibration

Although GOES instrumentation is similar on the different satellites in the series, observed fluxes are significantly different. For example, GOES-8 values are significantly lower than GOES-7 values. If these data sets are to be used together we need to examine whether these differences can be explained solely by the difference in L arising from the longitude displacement between the spacecraft.

For each day in march 1994 and 1995, GOES-7 mean flux for the 3-hour interval closest to noon local time was extracted (or the maximum of the fluxes in the two nearest intervals). Data during solar proton events were removed because of potential contamination. In addition, data for electron enhancements immediately following Solar Proton Events were removed because the characteristics of these enhancements may differ from typical enhancements. Local noon L-values were computed as a function of spacecraft longitude using the Tsyganenko 1989 model. To retain the best accuracy, the observed Kp values were used in the magnetic field model. The results, shown in Figure 3, demonstrated that there was a significant variation in peak flux with L.

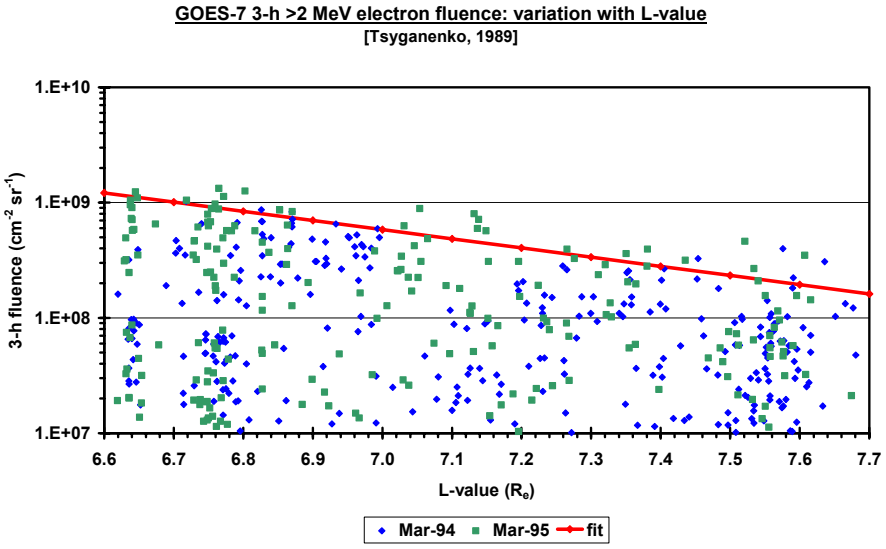

Figure 3. GOES-7 noon fluxes for March 1994 and 1995. A fit to the maximum fluxes is shown.

A straight line fit to the envelope of the GOES-7 data gives a suitable expression to translate all flux measurements to L= 6.6 equivalents: -

$$F_{6.6} = F_L \, 10^{(0.7955\,L\,-5.25)}$$

There were good data simultaneously from both GOES-7 and GOES-8 spacecraft between 1 June 1995 and 30 April 1996. Using the above equation, these data were translated to L=6.6. The results, shown in Figure 4, indicate that GOES-8 measurements can be normalised to GOES-7 equivalents by application of the following expression:-

$$F_{G7} \text{ equivalent} = 10^{(1.22 \log [FG8] - 1.463)}$$

REM/GOES cross-calibration

The STRV-1b and GOES spacecraft inhabit similar L and B/B_0 locations when STRV-1b is near to apogee. Hence a comparison between the fluxes at these times is possible if one uses a realistic magnetic field model to remove local time effects. Using REM data that had been processed to include the detector response for an exponential spectrum [private communication, Buehler], the >2MeV flux can be inferred. A comparison for one day of a long-lived enhancement is shown in Figure 5. This shows good agreement between GOES-7 and REM. Over a longer period there are some differences but overall the two data sets are comparable (see Figure 6)

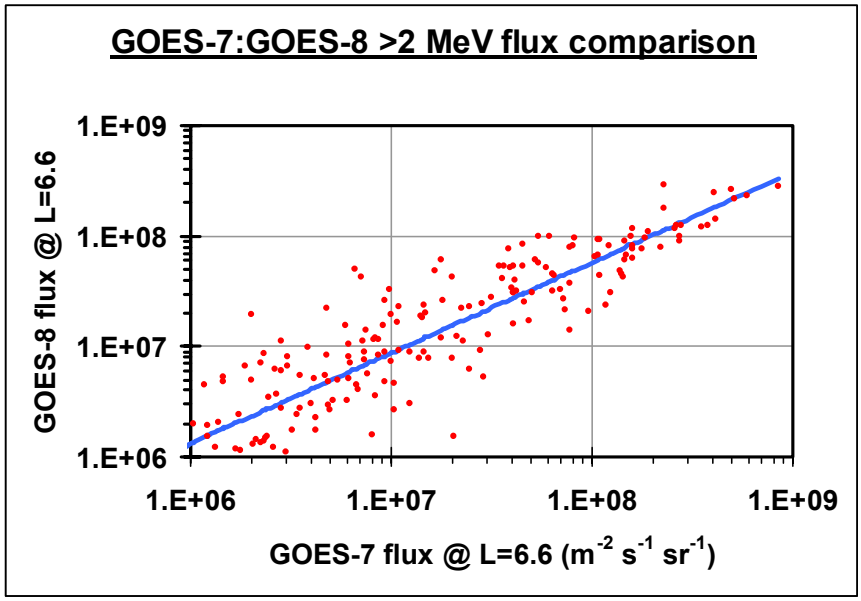

Figure 4. Comparison of GOES-7 and GOES-8 fluxes transformed to L=6.6.

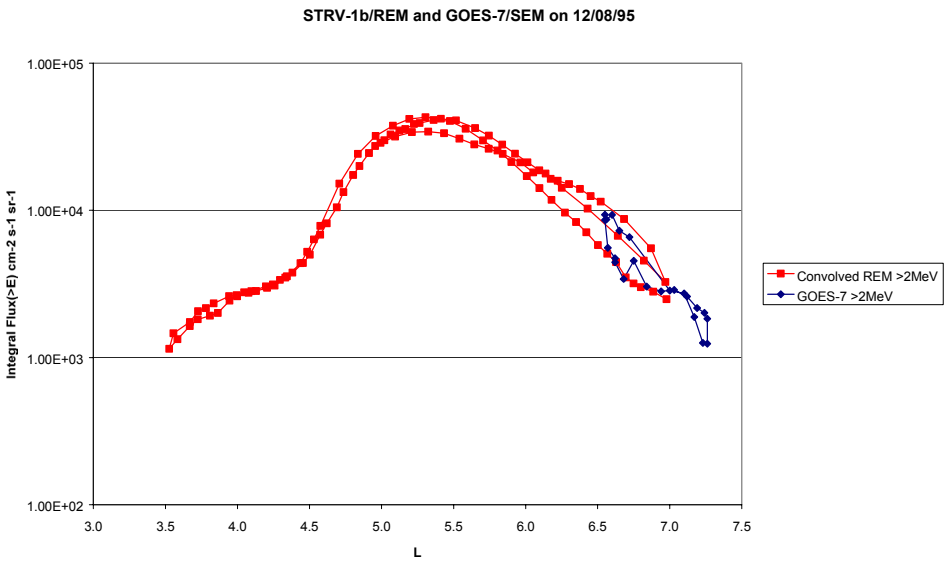

Figure 5. Comparison of convolved REM data and GOES L-profiles for a single day.

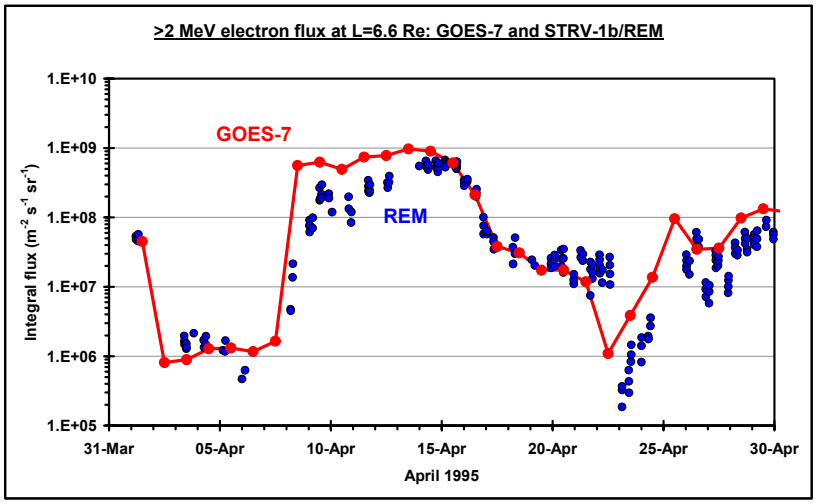

Figure 6. REM >2 MeV flux compared to GOES measurements at L=6.6 for April 1995

Modelling approach

Using magnetic field models to remove field-associated dependencies

Variations in the solar wind (i.e. speed, density and magnetic field) cause two separate effects that control observed energetic electron flux in the outer belt:

1. As a direct consequence of the field line motion, a spacecraft will sample different L shells; e.g. dropouts appear in flux in GEO as the field becomes more tail-like and the satellite effectively moves to higher L values.
2. The solar wind causes depletion and regeneration of the outer belt by whatever, poorly understood, processes occur – perhaps by injection, radial diffusion and acceleration, or wave particle interactions.

The first factor can be taken into account by a flux model in B/B0-L space if the adopted magnetic field model reliably reflects the existing level of geomagnetic activity. Models such as Olson-Pfitzer [10], Tsyganenko 1989 [9], and Tsyganenko 1996 [11], attempt to do this. The second factor must be modelled explicitly in the environment model. Using an activity-dependent model to determine L, might seem to negate the advantage of adopting the B/B0-L space framework, since geomagnetic activity cannot be an input when the model is used to estimate fluxes at future times. However, the long time-scales associated with internal charging help. The flux averaged over a day or more are heavily weighted by those intervals when the geomagnetic field was not greatly distorted, except for some periods with exceptional activity and then the intensities are normally low. Using a quiet-time (Kp=0) model errs on the conservative side. Modelling with a realistic magnetic field model therefore takes account of the asymmetry of the geomagnetic field involving orbit plane, longitude, local time and season.

Flux Envelopes

Because of the dynamically changing nature of the outer belt, a single B/B0-L co-ordinate may have widely differing flux at different times. Even during a single enhancement, the position of peak flux moves significantly, generally starting at high L and moving to lower L as the enhancement evolves [13]. An example is shown in Figure 7 for an enhancement in April 1995. This means that it is not sensible to select an outer belt profile from a single severe case but it is better to choose a flux profile that encompasses the range of outer belt profiles. This produces a conservative model that is applicable to all enhancements.

The occurrence rate of different flux levels is shown in Figure 8, for one channel of the REM data. This distribution has a steep upper boundary. Since FLUMIC seeks to give severe fluxes, it is this upper boundary that is modelled.

Spectrum

A convenient spectral shape for the outer belt is given by an exponential function, i.e.:

Flux $\propto$ $\exp(-E/E_0)$ where E is energy and E_0 is the e-folding energy

The small number of energy channels in the GOES/SEM and REM instruments does not justify a more complicated expression than this. It has been observed in geostationary orbit [10], that there is a link between flux enhancements at >2MeV and a hardening of the spectrum. However, REM data show that E_0 has no clear dependence on >1MeV flux. These two results are not necessarily contradictory but this issue warrants further investigation. REM data show that E_0 is quite constant in the outer belt, if one selects only >1MeV fluxes close around the flux 'envelope'. This is shown in Figure 9.

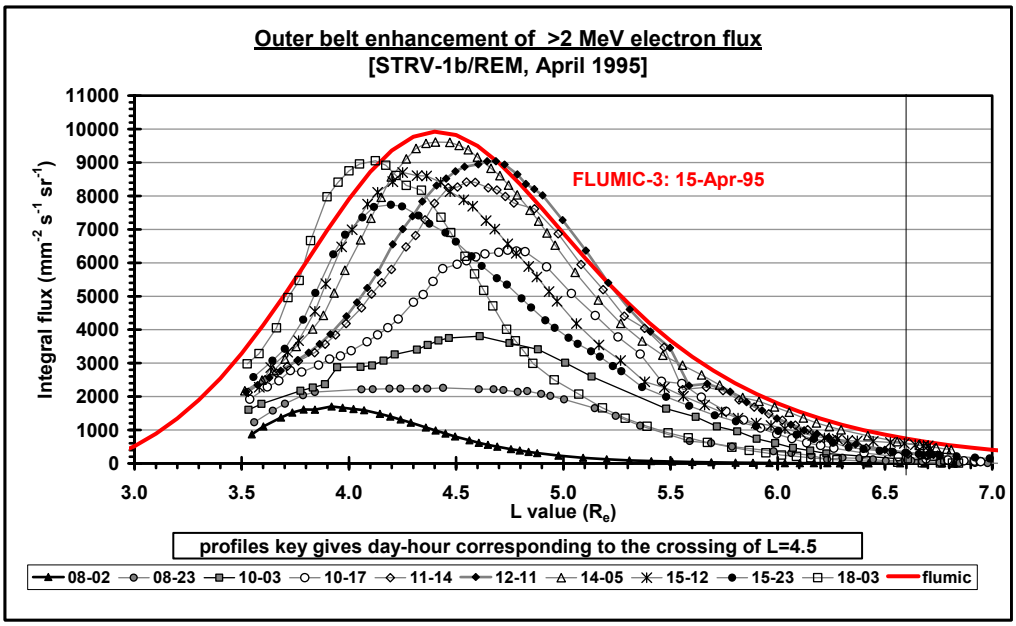

Figure 7. REM outer belt flux profiles over a 10-day period from 8th to 18th April 1995. Geostationary fluxes (marked by a line at L=6.6) are only weakly indicative of the behaviour of the belt as a whole. The FLUMIC3 'envelope' is shown.

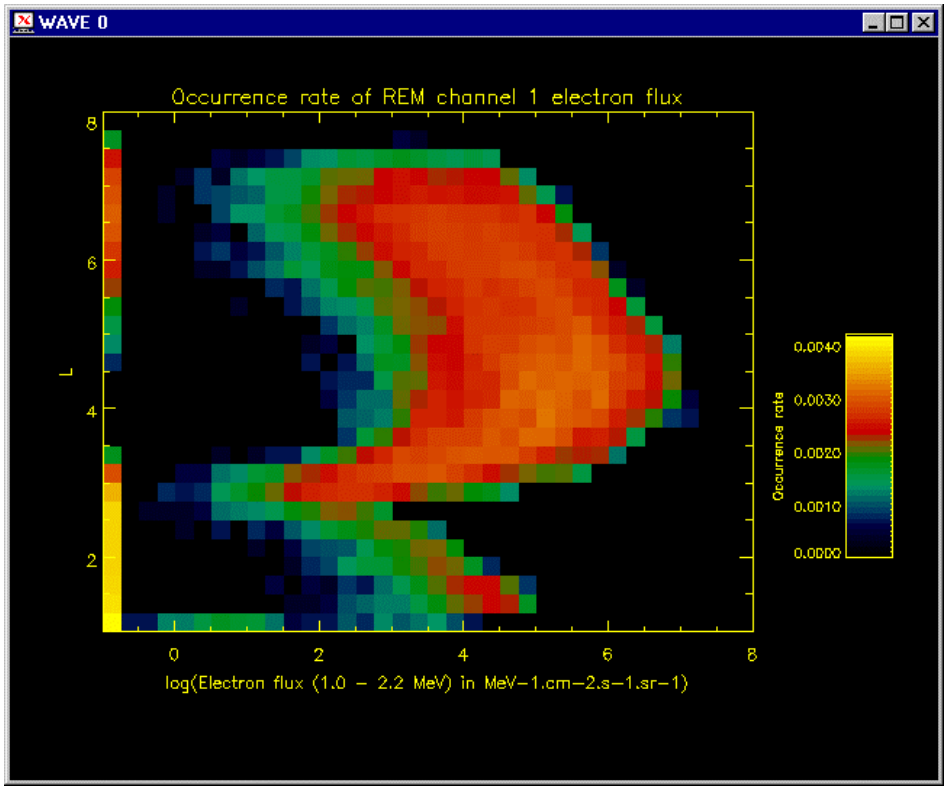

Figure 8. Distribution of flux values in the REM 1 to 2.2MeV channel.

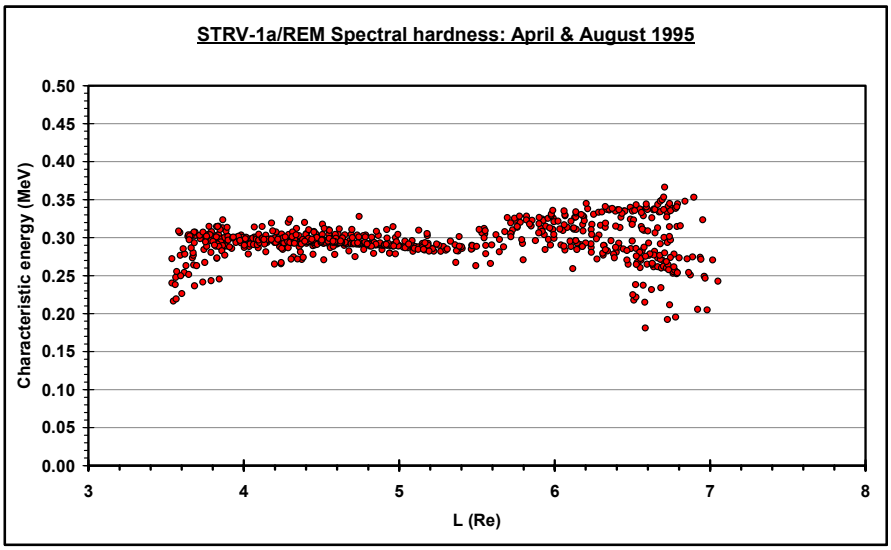

Figure 9. E_0 calculated from REM data, for times when >1MeV flux is more than 50% of the maximum for that L. L bins of width 0.2 were used.

In the inner belt, REM data in higher energy channels suffer some contamination from protons and so SURF data are used as the primary source of E_0. This is possible, despite the short time span of data from this instrument, because REM data show the inner belt fluxes to be very stable over long periods. SURF data show that E_0 is almost constant where fluxes are high and so a constant value of E_0 is a reasonable approximation.

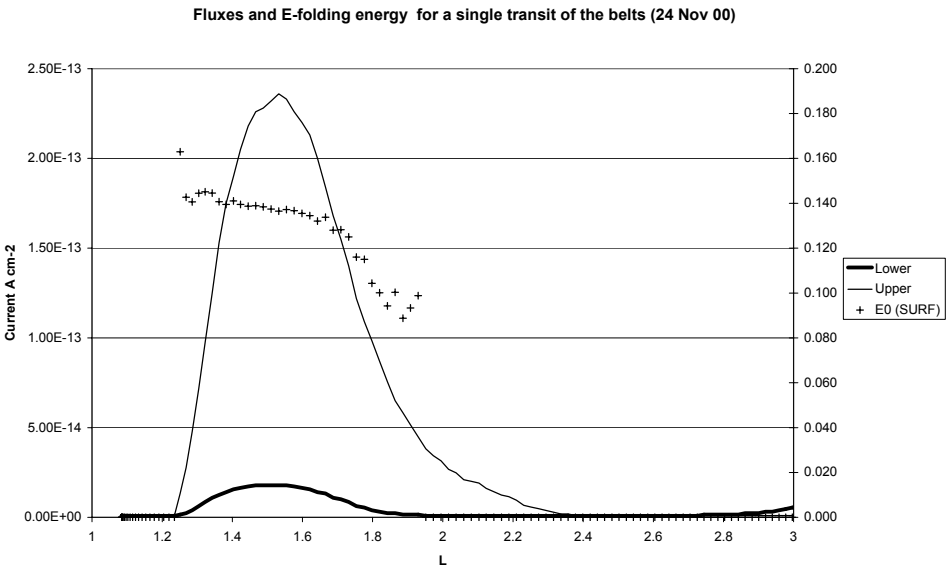

Figure 10. Current density measured in the SURF upper and lower plates for a crossing of the inner belt. The calculated value of E_0 is also shown.

Solar Cycle variation

The outer belt exhibits a strong solar cycle variation, with a peak in the declining phase of the sunspot cycle. Monthly maximum GOES >2MeV fluxes are shown in Figure 11 below. A curve approximately encompassing the peak fluxes is shown.

Seasonal variation

The seasonal variation of flux may be examined with the same GOES >2MeV data. As is shown in Figure 12 there are minima near the start and middle of the year, in agreement with previous observations of enhancements near the equinoxes. A simple curve is used to describe the variation in peak fluxes.

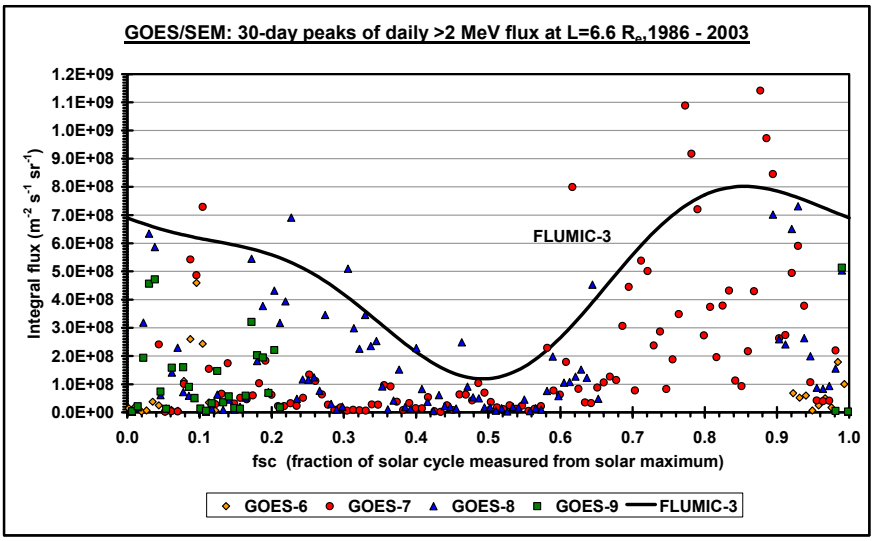

Figure 11. Solar Cycle variation of >2MeV electron flux for 1986-2003, normalised to GOES-7 fluxes at L=6.6, plotted against solar cycle phase (fsc). A curve encompasses almost all the enhancements.

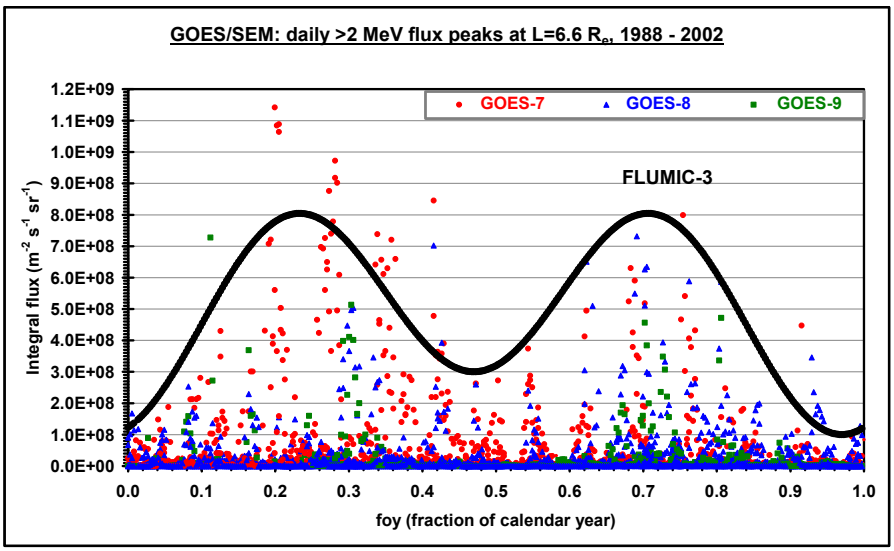

Figure 12. Daily >2MeV flux, plotted against fraction of calendar year (foy).

FLUMIC3 Equations Summary

The equations that comprise FLUMIC3 are shown below. These are currently in draft form.

OUTER BELT (L>2.5 R_e)

>2MeV Flux at L=6.6 R_e

The peak integral flux above 2 MeV at L= 6.6 is taken to be 8×10^8 m^{-2} s^{-1} sr^{-1}.

Solar Cycle

$F(fsc) = 8 \times 10^8 \{0.625 + 0.375 \sin[2\pi*(fsc-0.7)] + 0.125 \sin[4\pi*(fsc-0.15)]$

where *fsc* is the solar cycle phase starting at solar minimum.

Season

$F(foy,fsc) = F(fsc)\{0.625 - 0.375 \cos[4\pi(foy+0.03)] - 0.125 \cos[2\pi(foy+0.03)]\}$

where *foy* is the fraction of year starting from 1st January.

Spectrum

$F(>E) = F(>2MeV) \times \exp[(2-E)/E_0]$ where

$E_0 = 0.25$ for $F(>2MeV) < 10^7$ m^{-2} s^{-1} sr^{-1}.

$E_0 = 0.25 + 0.11((\log[F(>2MeV)] - 7)^{1.3})$ for $F(>2MeV) > 10^7$ m^{-2} s^{-1} sr^{-1}.

E_0 in the outer belt is the subject of ongoing study and so this aspect of the model may be updated before the model is finalised.

Flux versus L profile

$F(>E,L) = F(>E,6.6) \times 16\tanh[0.6(L-2.5)]/\cosh[1.5(L-4.3)]$ m^{-2} s^{-1} sr^{-1}

where $F(>E,6.6) = F(foy,fsc) \times \exp[(2-E)/E_0]$.

INNER BELT (L<2.5 R_e)

>1MeV Flux versus L profile

$F(>1MeV,L) = 4.0 \times 10^{\{2.12+45.4/(L+0.05)^2 - 45.6/(L+0.05)^3\}}$ $m^{-2}\ s^{-1}\ sr^{-1}$

Spectrum

$F(>E)=F(>1MeV) \times \exp[(1-E)/E_0]$

where $E_0 = 0.14$ MeV

B/B0

For $L < 3$ $Flux = Flux(equatorial) \times 10^{(-a((B/B0)-1))}$

where $a = -0.4559L+1.4385$ $L \geq 1.75$

and $a = 36.(1/\sinh((L-1)\times 10.)+0.7)$ $L<1.75$

For $L \geq 3$ the formula of Vette [14] is used, as in AE8

Acknowledgments

The authors are indebted to: Dr. Paul Buehler of the Paul Scherrer Institute, Switzerland; and Dr. Terry Onsager of NOAA/SEC for use of STRV-1b/REM and GOES/SEM data and assistance with their interpretation. This work was carried out as part of an ESA contract no. 16265/02/NL/FM under the direction of John Sørensen and we acknowledge his helpful comments on this work.

References

1. Whittlesey, A. Ed., NASA Technical Handbook, "Avoiding Problems Caused by Spacecraft On-Orbit Internal Charging Effects", NASA-HDBK-4002, Feb. 1999.

2. Wrenn, G.L., D.J.Rodgers & K.A.Ryden, "A solar cycle of spacecraft anomalies due to internal charging", Ann. Geophys. 20, 953-956, 2002.

3. Rodgers D.J., K.A.Ryden, P.M.Latham, L.Levy, 'Engineering Tools for Internal Charging: Final Report', ESA contract 12115/96/NL/JG(SC), Aug. 1998

4. Rodgers D.J., K.A.Ryden, P.M.Latham, G.L.Wrenn (T.S.Space Systems), L.Lévy, B.Dirassen , Engineering Tools for Internal Charging: Final Report', ESA contract 12115/96/NL/JG(SC) WO.1, CCN1, March 2000

5. Rodgers D.J, K.A.Ryden, G.L.Wrenn, P.M.Latham, J. Sørensen and L.Levy 'An Engineering Tool for the Prediction of Internal Dielectric Charging', Proceedings 6th Spacecraft Charging Technology Conference, 1998.

6. GOES I-M Databook, 19 November 2001 edition, http://rsd.gsfc.nasa.gov/goes/text/goes.databook.html

7. P.Buehler, S.Ljungfelt, A.Mchedlishvili, N.Schlumpf, A.Zehnder, L.Adams, E.Daly and R.Nickson; Radiation environment monitor, Nucl. Instr. and Meth. in Phys. Res. A,368, pp. 825-831, 1996.

8. Ryden,K.A., P.A.Morris, A.D.Fydland, H.S.Jolly, D.J.Rodgers, C.S.Dyer, "Profiles of inner- and outer- belt internal charging currents against geomagnetic parameter 'L': results from the first SURF experiment", Proc. 7th Spacecraft Charging Technology Conf., ESA-ESTEC, Noordwijk, April 2001.

9. Tsyganenko, N. A., A magnetospheric magnetic field model with a wrapped tail current sheet, Planet. Space Sci., 37, 5-20, 1989.

10. Olson, W. P., and K. A. Pfitzer, Magnetospheric magnetic field modeling, Annual Scientific Report, AFOSR Contract No. F44620-75-C-0033, 1977.

11. Tsyganenko, N. A., and D. P. Stern, Modeling the global magnetic field the large-scale Birkeland current systems, J. Geophys. Res., 101, 27187-27198, 1996.

12. Desorgher, L., P.Bühler, A. Zehnder, E.Daly, L.Adams, Variations of the outer radiation belt during the last two years, SP-392, p137,1996.

13. Wrenn, G.L., Rodgers, D.J., and Buehler, P.: "Modeling the outer belt enhancements of penetrating electrons", J. Spacecraft and Rockets 37, 408-415, 2000.

14. Vette, J.I., The AE-8 Trapped Electron Model Environment, NSSDC report 91-24, November 1991.